

October 22, 2018

$\alpha\alpha$ Scattering in Halo Effective Field Theory

R. Higa^{*} and H.-W. Hammer[†]

*Helmholtz-Institut für Strahlen- und Kernphysik,
Universität Bonn, 53115 Bonn, Germany*

U. van Kolck[‡]

Department of Physics, University of Arizona, Tucson, AZ 85721, USA

*Kernfysisch Versneller Instituut, Rijksuniversiteit Groningen,
Zernikelaan 25, 9747 AA Groningen, The Netherlands and*

*Instituto de Física Teórica, Universidade Estadual Paulista,
Rua Pamplona 145, 01405-900 São Paulo, SP, Brazil*

Abstract

We study the two-alpha-particle ($\alpha\alpha$) system in an Effective Field Theory (EFT) for halo-like systems. We propose a power counting that incorporates the subtle interplay of strong and electromagnetic forces leading to a narrow resonance at an energy of about 0.1 MeV. We investigate the EFT expansion in detail, and compare its results with existing low-energy $\alpha\alpha$ phase shifts and previously determined effective-range parameters. Good description of the data is obtained with a surprising amount of fine-tuning. This scenario can be viewed as an expansion around the limit where, when electromagnetic interactions are turned off, the ^8Be ground state is at threshold and exhibits conformal invariance. We also discuss possible extensions to systems with more than two alpha particles.

PACS numbers: 21.45.-v, 21.60.Gx

Keywords: Effective field theory, nuclear clusters

^{*}Electronic address: higa@itkp.uni-bonn.de

[†]Electronic address: hammer@itkp.uni-bonn.de

[‡]Electronic address: vankolck@physics.arizona.edu

I. INTRODUCTION

Nucleons in light nuclei have typical momenta that are small compared to the characteristic QCD scale of 1 GeV. At these low momenta, QCD can conveniently be represented by a hadronic theory containing all possible interactions consistent with the QCD symmetries. Effective Field Theory (EFT) provides a controlled framework for exploiting the separation of scales in nuclei. It is crucial to formulate a power counting that justifies a systematic truncation of the Lagrangian leading to observables with the desired accuracy. Nuclei offer a non-trivial challenge because one wants such a perturbative expansion in addition to the non-perturbative treatment of certain leading operators, which is required by the existence of shallow bound states. By now, mainly few-body systems have been studied within EFT, and, while much remains to be understood, many successes have been achieved [1, 2].

Similar to other approaches, the extension of EFTs to larger nuclei faces computational challenges [3, 4]. As a first step in this extension, we specialized to very low energies where clusters of nucleons behave coherently [5, 6, 7]. Even though many interesting issues of nuclear structure are by-passed, we can describe anomalously shallow (“halo” or “cluster”) nuclei and some reactions of astrophysical interest. Since they are strongly bound, alpha particles play a central role in this framework. Many nuclear states have energies close to thresholds for break-up into alpha particles and nucleons, the most famous being the excited (“Hoyle”) state of ^{12}C near the triple-alpha (3α) threshold. These states should be describable within the halo/cluster EFT, which is formulated with contact interactions among nucleon (N) and alpha-particle (α) fields. Together with the $N\alpha$ interaction, the $\alpha\alpha$ interaction is an important input for such calculations. While we have studied the $N\alpha$ interaction elsewhere through both neutron-alpha ($n\alpha$) [5, 6] and proton-alpha ($p\alpha$) [7] scattering, we focus here on $\alpha\alpha$ scattering. Consideration of this system is required before tackling other states with two or more alpha particles, such as ^9Be and ^{12}C .

The internal alpha-particle dynamics is characterized by an intrinsic momentum scale M_{hi} associated with the binding mechanism. A naive guess is that this scale is set by the pion mass $m_\pi \simeq 140$ MeV. The $\alpha\alpha$ interaction consists of the long-range photon exchange and short-range strong interactions. At low energies, the latter can be represented by contact interactions. The central issue is the relative importance of these contributions. The Coulomb interaction is non-perturbative for momenta smaller than around $k_C = Z_1 Z_2 \alpha_{em} \mu$, where $\alpha_{em} = e^2/4\pi$ is the fine-structure constant, μ the reduced mass of the system, and Z_i , $i = 1, 2$, the electromagnetic charge of the particles. Here $\mu = m_\alpha/2$ and $Z_i = Z_\alpha = 2$ in terms of the mass and charge of the alpha particle, respectively, so $k_C \approx 60$ MeV. At momenta much below 100 MeV, the deviation from pure-Coulomb $\alpha\alpha$ scattering is dominated by the S wave [8, 9, 10, 11, 12, 13, 14, 15]. The large near-threshold S -wave phase shift has been interpreted as resulting from a $(J^\pi, I) = (0^+, 0)$ state [14, 15, 16, 17, 18] at an energy $E_R \simeq 0.1$ MeV above threshold in the center-of-mass frame, with a tiny width $\Gamma_R \simeq 6$ eV. The momentum corresponding to this ^8Be state sets a smaller scale $M_{lo} \sim k_R = \sqrt{2\mu E_R} \approx 20$ MeV, which must arise from the larger underlying scale M_{hi} by a fine-tuning of the parameters of the underlying theory.

In the halo EFT, our goal is not to explain the mechanism of this fine-tuning, but instead to exploit its existence in order to describe α -cluster systems at low energies. We seek a description of these systems in an expansion in powers of the small ratio M_{lo}/M_{hi} . Power counting is dependent on how the various parameters scale with M_{lo} and M_{hi} . The physics of the low-energy S state is conveniently discussed in the language of a dimeron field [19]

with the quantum numbers of the low-energy composite state. This field is characterized in leading order by a fine-tuned mass Δ and a non-derivative coupling g to the $\alpha\alpha$ state. In subleading orders more complicated couplings appear.

It is not immediately obvious how the fine-tuned mass Δ relates to M_{lo} . The simplest assumption is $\Delta \sim M_{lo}M_{hi}/\mu$ [20]. In the absence of Coulomb interactions, this reproduces the leading term in the effective-range expansion, and one has a shallow real or virtual bound state with a typical momentum $k_B \sim M_{lo}$. Strong interactions are non-perturbative for momenta of order k_B and larger. Higher-order terms in the effective-range expansion appear as subleading corrections. This scenario is appropriate for S -wave NN scattering at momenta below $M_{hi} \sim m_\pi$ [21, 22]. For pp scattering, $k_B \approx 8$ MeV and $k_C \approx 4$ MeV. The Coulomb interaction can be included non-perturbatively in a straightforward way [23], providing calculable contributions plus a renormalization of Δ/g^2 .

The situation in $\alpha\alpha$ scattering is somewhat different. The extremely low energy of the S -wave resonance suggests that a smaller Δ might be necessary. An alternative fine-tuning assumes thus that $\Delta \sim M_{lo}^2/\mu$. Such scaling has already appeared in P -wave $N\alpha$ scattering [5, 6], and has striking consequences in S -wave $\alpha\alpha$ scattering. In the absence of the Coulomb interaction, the leading contribution for momenta $k \sim M_{lo}$ comes entirely from the unitarity term $-ik$ in the inverse amplitude. To this order, the ${}^8\text{Be}$ system would be at the so-called unitary limit, exhibiting conformal invariance [24, 25], and ${}^{12}\text{C}$ would acquire an exact Efimov spectrum [2, 25, 26]. As we will discuss later, this exact pattern is modified by the Coulomb interaction, which breaks scale invariance and thus moves the ${}^8\text{Be}$ ground state away from threshold. We will see that in leading order we can describe the ground state, and higher-energy, scattering data can be systematically accounted for in higher orders. At this point, we simply fit the EFT parameters to data. In the future, many-body methods [3, 4] should allow the calculation of these parameters from the underlying EFTs, which in turn will have their parameters obtained from lattice QCD [27].

To the extent that the halo/cluster EFT is built on fields for clusters, it is closely related to phenomenological few-body cluster models [14, 28]. The latter have had many applications, ranging from the general analysis of halo structures [29] to the successful confrontation with data for specific processes, such as decays of ${}^{12}\text{C}$ resonances [30]. The emphasis here is instead on a systematic expansion of the most general interactions allowed by the symmetries of QCD.

In this paper, we study the alternative expansion scenario and perform a detailed comparison to phase-shift data for the $\alpha\alpha$ system. As we will see, among the many findings our new method entails are a new expansion for the $\alpha\alpha$ amplitude around the resonance, which differs from the effective-range expansion; the existence of inconsistencies between recent resonance measurements and old scattering data; a more precise determination of low-energy parameters; and an extraordinary amount of fine-tuning. All these findings could have implication in the study of other alpha-cluster systems. The paper is organized as follows. In Sec. II, we briefly discuss the EFT formulation of the two-body system with Coulomb interactions, with some details relegated to App. A. The proposed power counting is discussed in Sec. III. In Sec. IV, we present results of our fits to the 0^+ resonance parameters and $\alpha\alpha$ phase shifts, and discuss the required fine-tunings. Our conclusions are presented in Sec. V.

II. EFT WITH COULOMB INTERACTIONS

We start with a summary of some basic ideas in halo EFT [5, 6, 7], extended to include the main equations needed to deal with Coulomb interactions. These equations are a straightforward generalization of Kong and Ravndal’s formalism [23] to include dimeron fields¹. More details can be found in App. A. In Sect. III we discuss the significant differences in scales between alpha-cluster systems and the pp system considered by Kong and Ravndal [23].

We consider here the scattering of two alpha particles of charge $Z_\alpha = 2$ and reduced mass $\mu = m_\alpha/2$, at a center-of-mass (CM) energy $E = k^2/2\mu$. We want to build an EFT that provides a controlled expansion for observables at momenta around the 0^+ resonance, $k \sim k_R = \sqrt{2\mu E_R} \approx 20 \text{ MeV} \sim M_{l_o} \ll M_{hi}$. The energy of the resonance, $E_R \simeq 0.1 \text{ MeV}$, is much smaller than either the alpha-particle excitation energy $E_\alpha^* \simeq 20 \text{ MeV}$ or any energy set by pion exchange, such as two-pion exchange between alpha particles or one-pion exchange among nucleons, $(2m_\pi)^2/m_\alpha \sim m_\pi^2/m_N \approx 20 \text{ MeV}$. Thus, we expect an alpha particle to behave in a first approximation as a rigid entity (“core” or “cluster”), which we represent by a scalar-isoscalar field ϕ . The smaller effects from deformations and other core-structure properties are accounted for in a derivative expansion. The breakdown momentum scale M_{hi} of this EFT will be set by the lowest-energy degrees of freedom that are not incorporated explicitly in the Lagrangian. Since these include the nucleons within the alpha particle—which can be resolved with a momentum $\sqrt{m_N E_\alpha^*} \approx 140 \text{ MeV}$ —and the pions—which can be resolved with momenta of the order of the pion mass $m_\pi \simeq 140 \text{ MeV}$ —a reasonable estimate is $M_{hi} \sim \sqrt{m_N E_\alpha^*} \sim m_\pi \simeq 140 \text{ MeV}$. The EFT provides an expansion of observables in powers of the ratio between the low-energy scales k and M_{l_o} and the high-energy scale M_{hi} .² Around the resonance $k \sim k_R$, we expect an expansion parameter of the order of $1/7$. As the energy increases the expansion deteriorates and one should not expect the EFT to be applicable to laboratory (LAB) energies much above $E_{LAB} = k^2/\mu \sim 3 \text{ MeV}$, a conservative estimate that corresponds to a CM momentum of about 70 MeV .

Since at low energies only S waves contribute significantly to $\alpha\alpha$ scattering beyond pure Coulomb scattering, we introduce an auxiliary scalar dimeron field d with “residual mass” Δ , which couples to two α fields. (Observables are independent of the choice of fields.) We thus start with the following strong-interaction effective Lagrangian:

$$\mathcal{L} = \phi^\dagger \left[i\partial_0 + \frac{\nabla^2}{2m_\alpha} \right] \phi + \sigma d^\dagger \left[i\partial_0 + \frac{\nabla^2}{4m_\alpha} - \Delta \right] d + g \left[d^\dagger \phi \phi + (\phi \phi)^\dagger d \right] + \dots, \quad (1)$$

where $\sigma = \pm 1$ and g is a coupling constant. The “...” represent interactions with higher derivatives. The sign σ is used to match the sign of the effective range r_0 . The existence of

¹ A similar extension was recently considered by Ando and collaborators [33].

² Recently it has been suggested [31] that chiral symmetry is important for the properties of the ^8Be ground state. This argument is based on an extension of the halo EFT to include explicit pion fields. In fact, it had been pointed out before [32] that the long-range interaction of alpha particles is related to two-pion exchange, but in the context of nucleon scattering on an alpha particle built out of four nucleons. Since the pion mass is not much smaller than the typical nucleon momentum in the alpha particle, we see no rationale (for realistic values of the quark masses) for an expansion in powers of m_π/M_{hi} in a theory with “elementary” alpha particles.

this sign merely reflects the non-physical, auxiliary character of the dimeron field [19, 20]. In momentum space, associated with the displayed bilinear terms are the α propagator

$$i S_\alpha(q_0; \mathbf{q}) = \frac{i}{q_0 - \mathbf{q}^2/2m_\alpha + i\epsilon}, \quad (2)$$

and the dimeron propagator

$$i D_d(q_0; \mathbf{q}) = \frac{i \sigma}{q_0 - \mathbf{q}^2/4m_\alpha - \Delta + i\epsilon}. \quad (3)$$

Other terms in the Lagrangian (1) can be treated as insertions of interaction vertices in Feynman diagrams or corrections to the propagators (2) and (3).

Different assumptions about the dependence of Δ on M_{lo} translate into different relative weights for the terms in the denominator of Eq. (3), where $|\mathbf{q}| \sim \sqrt{2\mu q_0} = \mathcal{O}(M_{lo})$. For example, in the present scenario all terms are of the same size, while in the NN case the energy and kinetic terms are of subleading order and the dimeron propagator reduces in leading order to $i D_d \rightarrow -i\sigma/(\Delta - i\epsilon)$. (The latter form gives rise in the amplitude not to a resonance but to a bound-state pole [20] at a momentum $k_B = i/a_0$, where a_0 is given by Eq. (13).) In this section we illustrate the use of the Lagrangian (1) together with electromagnetic interactions to calculate $\alpha\alpha$ scattering amplitudes. We postpone a discussion of the relative importance of various terms until the next section.

Electromagnetic interactions are introduced into the effective Lagrangian (1) in the standard way, that is, by both changing the derivatives into gauge-covariant ones, and introducing gauge-invariant interactions generated by the electromagnetic field strength. For practical calculations one usually works in a fixed gauge. The Coulomb gauge is very convenient, since it allows a clear separation between Coulomb and transverse photons. The former provides the leading electromagnetic interaction and is driven by the Sommerfeld parameter

$$\eta(k) \equiv \frac{Z_\alpha^2 \alpha_{em} \mu}{k} = \frac{k_C}{k}, \quad (4)$$

with $\alpha_{em} \equiv e^2/4\pi$ the fine-structure constant and k_C the inverse of the “Bohr radius” of the $\alpha\alpha$ system. This parameter is enhanced by the presence of μ in the numerator, which, as we are going to see, makes η large around the resonance and requires a non-perturbative resummation of Coulomb photons. On the other hand, transverse photons are suppressed [1, 34] by two powers of M_{lo}/μ , and when in loops by extra powers of α_{em} . Since numerically $\mu \sim 2M_{hi}^2/M_{lo}$, these interactions contribute to orders—where they can be accounted for in perturbation theory—beyond the precision we are working with. They can become significant only at energies comparable to the excitation energy of the α core.

The scattering amplitude for two particles interacting via Coulomb plus a short-range interaction is given by [35] (for more details, see App. A):

$$T = T_C + T_{CS}, \quad (5)$$

where T_C and T_{CS} are the pure-Coulomb and the Coulomb-distorted short-range amplitudes, respectively. Considering only S -wave interactions, the Coulomb-distorted short-range amplitude is parametrized in terms of the “Coulomb-corrected” phase shift δ_0^c as

$$T_{CS} = -\frac{2\pi}{\mu} \frac{e^{2i\sigma_0}}{k(\cot \delta_0^c - i)} = -\frac{2\pi}{\mu} \frac{C_\eta^2 e^{2i\sigma_0}}{2k_C [K(\eta) - H(\eta)]}, \quad (6)$$

with the pure-Coulomb phase shift σ_0 given by Eq. (A5) in the Appendix and the Sommerfeld factor

$$C_\eta^2 = \frac{2\pi\eta}{e^{2\pi\eta} - 1}. \quad (7)$$

The H function is given by Eq. (A15). For real η it can be expressed as

$$H(\eta) = \text{Re}[\psi(1 + i\eta)] - \ln \eta + \frac{i}{2\eta} C_\eta^2 \quad (8)$$

in terms of the digamma function $\psi(z) = (d/dz) \ln \Gamma(z)$. The other (real) term in the denominator of Eq. (6) is the Landau-Smorodinsky K function [37],

$$K(\eta) \equiv \frac{C_\eta^2}{2\eta} (\cot \delta_0^c - i) + H(\eta). \quad (9)$$

At low energies it reduces to the effective-range expansion (ERE) in the presence of Coulomb interactions,

$$K(\eta) = \frac{1}{2k_C} \left[-\frac{1}{a_0} + \frac{r_0}{2} k^2 - \frac{\mathcal{P}_0}{4} k^4 + \dots \right], \quad (10)$$

where $a_0, r_0, \mathcal{P}_0, \dots$, are the scattering length, effective range, shape, \dots , parameters.

As shown in App. A, the calculation using the EFT Lagrangian (1) leads to

$$T_{CS} = -\frac{2\pi}{\mu} C_\eta^2 e^{2i\sigma_0} \left[\sigma \frac{2\pi \Delta^{(R)}}{\mu g^2} - \sigma \frac{\pi}{\mu^2 g^2} k^2 - 2k_C H(\eta) \right]^{-1} + \dots, \quad (11)$$

where $\Delta^{(R)}$ is the Coulomb-renormalized mass parameter of the EFT Lagrangian,

$$\Delta^{(R)} = \Delta(\kappa) - \sigma \frac{\mu g^2}{2\pi} \left\{ \frac{\kappa}{D-3} + 2k_C \left[\frac{1}{D-4} - \ln \left(\frac{\sqrt{\pi}\kappa}{2k_C} \right) - 1 + \frac{3}{2} C_E \right] \right\}, \quad (12)$$

with κ the renormalization scale and D the dimension of spacetime. Equation (11) is in the form of the Coulomb-modified ERE with scattering length and effective range given respectively by

$$a_0 = -\sigma \frac{\mu g^2}{2\pi \Delta^{(R)}}, \quad r_0 = -\sigma \frac{2\pi}{\mu^2 g^2}. \quad (13)$$

From Eq. (11) it is clear that the effect of a non-perturbative Coulomb dressing of the strong-interaction amplitude —apart from multiplying the amplitude by $C_\eta^2 e^{2i\sigma_0}$ and from renormalizing the short-range parameters— is to effectively replace the unitarity term $-ik$ by $-2k_C H(\eta)$. In order to estimate the relative sizes of the various contributions to Eq. (11), we turn now to a discussion of power counting. As we are going to see, at each order the EFT in the two-body system is equivalent to a truncation of the Coulomb-modified ERE.

III. POWER COUNTING

In this section we elaborate on the proposed power-counting scenario mentioned in the Introduction. We also give the $\alpha\alpha$ amplitudes that are used in the next section for a comparison to phase-shift data.

In the present strongly-tuned scenario one considers $\Delta \sim M_{lo}^2/\mu$ and $g^2/2\pi \sim M_{hi}/\mu^2$, with other couplings scaling with M_{hi} according to naive dimensional analysis. In this case the contribution of the bare dimeron propagator to the scattering amplitude at momentum $k \sim M_{lo}$ comes not only from the dimeron mass, but also from its kinetic term. The simplest strong-interaction contribution is a bare dimeron propagator attached to initial and final external legs, which (as seen by multiplying Eq. (3) by g^2) is of $\mathcal{O}(2\pi M_{hi}/\mu M_{lo}^2)$. A non-Coulomb bubble diagram times another dimeron propagator brings an extra factor of $\mathcal{O}(\mu g^2 k/2\pi\Delta) = \mathcal{O}(M_{hi}/M_{lo})$. As a consequence, the bubble-chain resummation is necessary. The resulting denominator acquires the form $(-1/a_0 + r_0 k^2/2 - ik)$. Interesting in this power counting is the fact that at momenta $k \sim M_{lo}$ the first two terms are suppressed by M_{lo}/M_{hi} compared to the last one. Therefore, all that is left at LO if the Coulomb interaction is turned off is the unitarity term $1/(-ik)$. In this limit, the ^8Be system exhibits conformal invariance [24, 25] and the corresponding three-body system, ^{12}C , acquires an exact Efimov spectrum [2, 25, 26]. This scenario is a possible realization of the unitary limit.

This picture is significantly modified when the Coulomb interaction is turned on. In a non-relativistic system an $1/r$ potential breaks scale invariance and introduces the scale k_C in the propagation of two charged particles. As we have seen in Eq. (11), the unitarity term is modified. The balance between strong-interaction terms and Coulomb-modified propagation depends on both the intrinsic strong-interaction scale and k_C . We note that the scales are very different in $\alpha\alpha$ than in pp scattering. While for the latter $k_C/k_B \sim 1/2$, for the $\alpha\alpha$ system, $k_C = \alpha_{em} Z_\alpha^2 m_\alpha/2 \sim 60$ MeV and $k_R = \sqrt{m_\alpha E_R} \sim 20$ MeV, so $k_C/k_R \sim 3$. For momenta $k \sim k_R$, we are therefore in the deep non-perturbative Coulomb region.³ This case corresponds to large values of η , where the function $2k_C H(\eta)$ is significantly different from the usual unitarity term ik . Using Stirling's series [36],

$$\ln \Gamma(1+z) = \frac{1}{2} \ln 2\pi + \left(z + \frac{1}{2}\right) \ln z - z + \frac{1}{12z} - \frac{1}{360z^3} + \dots, \quad (14)$$

in Eq. (8) gives

$$H(\eta) = \frac{1}{12\eta^2} + \frac{1}{120\eta^4} + \dots + \frac{i\pi}{e^{2\pi\eta} - 1}. \quad (15)$$

The unitarity term is thus replaced by $2k_C H(\eta) \sim k^2/6k_C$. This term is now a factor $k/6k_C$ smaller in magnitude than the unitarity term in the absence of Coulomb, and comparable to the effective-range term coming from the dimeron kinetic term. This can be captured automatically if we take $3k_C \sim M_{hi}$, as it appears to be the case numerically.

If all higher-order parameters are natural, in the S wave the shape-parameter term $\mathcal{P}_0 k^4 = \mathcal{O}(M_{lo}^4/M_{hi}^3)$ is down by $(M_{lo}/M_{hi})^2$ compared to the effective-range term $r_0 k^2 = \mathcal{O}(M_{lo}^2/M_{hi})$, and so should be each of the successive terms. On the other hand, the D -wave scattering-“length” term $a_2 k^4 = \mathcal{O}(M_{lo}^4/M_{hi}^5)$ is down by $(M_{lo}/M_{hi})^6$ compared to the S -wave scattering length $a_0 = \mathcal{O}(M_{hi}/M_{lo}^2)$, and further energy dependence and higher angular momenta bring in further powers of $(M_{lo}/M_{hi})^2$.

In this power counting, the Coulomb-distorted short-range amplitude T_{CS} is given in LO

³ This fact suggests that one might be able to develop a perturbation scheme in powers of $k_R/k_C = 2\sqrt{E_R/m_\alpha}/\alpha_{em} Z_\alpha^2$.

by Eq. (11). Including corrections in perturbation theory, we obtain up to NLO:

$$T_{CS} = -\frac{2\pi}{\mu} C_\eta^2 e^{2i\sigma_0} \left[\frac{1}{-1/a_0 + k^2 r_0/2 - 2k_C H} + \frac{\mathcal{P}_0}{4} \frac{k^4}{(-1/a_0 + k^2 r_0/2 - 2k_C H)^2} \right], \quad (16)$$

where \mathcal{P}_0 is given by a higher-derivative term in the Lagrangian (1). This corresponds to an expansion of the ERE formula,

$$T_{CS}^{(\text{ERE})} = -\frac{2\pi}{\mu} \frac{C_\eta^2 e^{2i\sigma_0}}{-1/a_0 + k^2 r_0/2 - k^4 \mathcal{P}_0/4 - 2k_C H}, \quad (17)$$

for small \mathcal{P}_0 . To this order, all waves higher than S are purely Coulombic. Higher orders can be calculated similarly.

Equation (16) holds for generic momenta $k \sim M_{lo}$. However, it fails in the immediate proximity of k_R . This situation is familiar from another application of the halo EFT to a resonance [6]. The power counting works for $k \sim M_{lo}$ except in the narrow region $|k - k_R| = \mathcal{O}(M_{lo}^2/M_{hi})$ where the LO denominator nearly vanishes and a resummation of the NLO term, here associated with the shape parameter, is required. As one gets closer to the resonance momentum k_R , higher-order terms in the ERE are kinematically fine-tuned as well. This happens because the imaginary part of the denominator is exponentially suppressed by a factor $\exp(-2\pi\eta_R) \sim 10^{-8}$ and the real part gets arbitrarily small. (For $n\alpha$ scattering, multiple kinematical fine-tunings are prevented in the $P_{3/2}$ wave by the presence of an imaginary term $ik^3 \sim M_{lo}^3$ [5, 6].)

This kinematical fine-tuning is not a conceptual problem. From the EFT point of view, each new fine-tuning is equivalent to reshuffling the series and redefining the pole position. Such a procedure works fine with a small number of kinematical fine-tunings, but is not practical in the present case. A better alternative is to perform an expansion around the resonance pole position. The situation here is analogous to the NN system, where we can choose to expand the amplitude around the bound-state pole [22] rather than around zero energy.

A great simplification results from the fact that the resonance lies in the deep Coulomb regime, where Eq. (15) provides an accurate representation of H up to the precision we are considering. The real terms shown in Eq. (15) can be seen as an expansion in powers of $\sim (k/3k_C)^2 = \mathcal{O}(k^2/M_{hi}^2)$. Of course in an asymptotic expansion at some point the remaining terms can no longer be expanded; at that point the remainder should be treated exactly. In lowest orders, however, we can use the successive terms shown in Eq. (15): numerically, the terms up to η^{-4} work to better than 3% for $E_{LAB} = 3$ MeV.

The expansion (15) makes the physics around the resonance quite transparent. Since the “size” of the resonance, $1/k_R$, is much larger than the Bohr radius $1/k_C$, the Coulomb interaction is effectively short ranged, and the real part of H is ERE-like. This expansion matches well with the expansion for the Landau-Smorodinski function, which is in powers of $(k/M_{hi})^2$. In T_{CS} , not only the k^2 terms, but also higher-order terms from strong and Coulomb interactions have comparable sizes. We can thus lump these terms together, defining

$$\tilde{r}_0 = r_0 - \frac{1}{3k_C}, \quad \tilde{\mathcal{P}}_0 = \mathcal{P}_0 + \frac{1}{15k_C^3}, \quad (18)$$

and so on.

In this case we can rewrite up to NLO:

$$\begin{aligned}
T_{CS} &= -\frac{2\pi}{\mu} \frac{C_\eta^2 e^{2i\sigma_0}}{-1/a_0 + \tilde{r}_0 k^2/2 - \tilde{\mathcal{P}}_0 k^4/4 - ikC_\eta^2} \\
&= -\frac{2\pi}{\mu} \frac{C_\eta^2 e^{2i\sigma_0}}{\tilde{r}_0(k^2 - k_R^2)/2 - \tilde{\mathcal{P}}_0(k^4 - k_R^4)/4 - ikC_\eta^2} \\
&= -\frac{2\pi}{\mu} C_\eta^2 e^{2i\sigma_0} \left[\underbrace{\frac{1}{\tilde{r}_0(k^2 - k_R^2)/2 - ikC_\eta^2}}_{\text{LO term}} + \underbrace{\frac{\tilde{\mathcal{P}}_0}{4} \frac{(k^4 - k_R^4)}{(\tilde{r}_0(k^2 - k_R^2)/2 - ikC_\eta^2)^2}}_{\text{NLO correction}} + \dots \right], \quad (19)
\end{aligned}$$

where

$$k_R^2 = \frac{2}{a_0 \tilde{r}_0} \left(\underbrace{1}_{\text{LO term}} - \underbrace{\frac{\tilde{\mathcal{P}}_0}{a_0 \tilde{r}_0^2}}_{\text{NLO correction}} + \dots \right). \quad (20)$$

From this expression one sees directly that, indeed, $k_R \sim M_{lo}$, with corrections of $\mathcal{O}(M_{lo}^2/M_{hi}^2)$. Note that we keep the exact form of the imaginary term in Eq. (19): even though it is negligible at $k \sim k_R$, it has an important exponential dependence on the energy responsible for keeping the phase shifts real in the elastic regime.

When $a_0 < 0$ and $\tilde{r}_0 < 0$, and thus $r_0 < 1/3k_C$, we have $k_R^2 > 0$ and the two poles of Eq. (19) are located in the lower half of the complex-momentum plane very near the real axis, as befits a very narrow resonance. The amplitude T_{CS} can be written in terms of the resonance energy $E_R = k_R^2/2\mu$ and the resonance width $\Gamma(E)$ as

$$T_{CS} = \frac{2\pi e^{2i\sigma_0}}{\mu\sqrt{2\mu E}} \frac{\Gamma(E)/2}{E - E_R + i\Gamma(E)/2}. \quad (21)$$

One finds that

$$\Gamma(E) = \Gamma(E_R) \frac{e^{2\pi k_C/k_R} - 1}{e^{2\pi k_C/k} - 1} \left[\underbrace{1}_{\text{LO term}} - \underbrace{\frac{\mu^2 \tilde{\mathcal{P}}_0}{2\pi k_C} (e^{2\pi k_C/k_R} - 1) \frac{\Gamma(E_R)}{2} (E - E_R) + \dots}_{\text{NLO correction}} \right], \quad (22)$$

where

$$\Gamma(E_R) = -\frac{4\pi k_C}{\mu \tilde{r}_0} \frac{1}{e^{2\pi k_C/k_R} - 1} \left(\underbrace{1}_{\text{LO term}} + \underbrace{\frac{\tilde{\mathcal{P}}_0 k_R^2}{\tilde{r}_0}}_{\text{NLO correction}} + \dots \right). \quad (23)$$

The width is very small because of the large value of $2\pi k_C/k_R$ in the exponential.

In the form of Eqs. (21) and (22) we can keep E_R and $\Gamma(E_R)$ fixed at each order in the expansion. Note that these equations do not change to this order if one makes a different choice —*e.g.*, $(k^2 - k_R^2)^2$ instead of $k^4 - k_R^4$ — for the form of the $\tilde{\mathcal{P}}_0$ term in Eq. (19). Since at the resonance, $\delta_0^c(E_R) = \pi/2$ and $[d\delta_0^c(E)/dE]_{E_R} = 2/\Gamma(E_R)$, the behavior of the phase shift around E_R is fixed. We turn now to a test of the expansion (19) mandated by our power counting.

IV. COMPARISON TO DATA

In this section we briefly describe the experimental situation regarding $\alpha\alpha$ scattering at low energies. Our predictions are then compared against the available data and discussed in detail, with a particular emphasis on the scalings of the EFT parameters.

Scattering data at low energies are not abundant. At energies below $E_{LAB} = 3$ MeV data were obtained, and a phase-shift analysis performed, in Ref. [8]. All later references that we were able to find [14, 15] start at higher energies. For example, Ref. [9] covers the region $E_{LAB} = 3$ –6 MeV, Ref. [10] $E_{LAB} = 3.8$ –12 MeV, and Ref. [11] $E_{LAB} = 5$ –9 MeV. These data show that $\alpha\alpha$ scattering at $E_{LAB} \lesssim 6$ MeV is dominated by the S wave, thanks to the presence of a $(J^\pi, I) = (0^+, 0)$ resonance immediately above threshold, identified as the ^8Be ground state [15]. Early determinations of the 0^+ resonance energy were performed in reactions like $^{11}\text{B} + p \rightarrow 2\alpha + \alpha$ [16]. Later measurements and careful analysis of the scattering of ^4He atoms off $^4\text{He}^+$ ions [17, 18] improved the determination of the resonance energy and width to their currently accepted values, $E_{LAB}^R = 184.15 \pm 0.07$ keV and $\Gamma_{LAB}^R = 11.14 \pm 0.50$ eV. The resonance CM momentum is thus $k_R = \sqrt{\mu E_{LAB}^R} \approx 18.5$ MeV. At $E_{LAB} \approx 6$ MeV the D -wave phase shift crosses $\pi/2$, indicating the position of a broader resonance associated with the first excited, $(2^+, 0)$ state [15]. The G wave does not become comparable to the D wave until $E_{LAB} \sim 20$ MeV, interpreted as the region of an even broader $(4^+, 0)$ state [15].

The low-energy data can be studied with the ERE. When used together with the 0^+ resonance energy [16], the data from Refs. [8, 9] give for these parameters [9]: $a_0 = -1.76 \times 10^3$ fm, $r_0 = 1.096$ fm, and $\mathcal{P}_0 = -1.654$ fm³. They provide a good description of the available phase shifts up to $E_{LAB} \approx 6$ MeV, which lends some credence to these numbers. However, it was pointed out [12] that without input from the 0^+ resonance width these parameters have large uncertainties. Inclusion of both resonance energy and width from Ref. [17] reduces these uncertainties considerably [13]: $a_0 = (-1.65 \pm 0.17) \times 10^3$ fm, $r_0 = (1.084 \pm 0.011)$ fm, and $\mathcal{P}_0 = (-1.76 \pm 0.22)$ fm³. Since the later, more precise data from Ref. [18] are consistent with Ref. [17], the ERE parameters from Ref. [13] can be seen as a reasonable parametrization of the existing data.

Here we use the phase shifts compiled in Table II of Ref. [14]. Since it is well-determined experimentally, and due to its relevance to the triple-alpha process, we use the 0^+ state as an important constraint. This is in line with the EFT approach, where lower-energy observables have smaller theoretical errors. It provides a relationship among our EFT parameters and, consequently, reduces the number of variables to be adjusted at each order in the power counting. Below, we also use the ERE from Ref. [13] for orientation, and comment on the extremely large value of the scattering length a_0 , which suggests a large amount of fine-tuning in the parameters of the underlying theory away from the naturalness assumption. In contrast, both $r_0^{-1} \sim 180$ MeV and $\mathcal{P}_0^{-1/3} \sim 170$ MeV correspond to natural scales comparable to the pion mass. At this level there is no evidence against our initial estimate of the expansion parameter $M_{lo}/M_{hi} \sim 1/7$. Note that here we do not include dimeron fields for resonances beyond the ground state, and therefore cannot go beyond the energy region where the D -wave resonance is significant.

In the power counting we are proposing for the $\alpha\alpha$ system, the amplitude T_{CS} for generic momenta is given up to NLO by Eq. (19). As previously discussed, this expression combines the deep-non-perturbative Coulomb approximation (15) for the function H with the expansion around the resonance pole, which avoids the need for multiple kinematical fine-tunings.

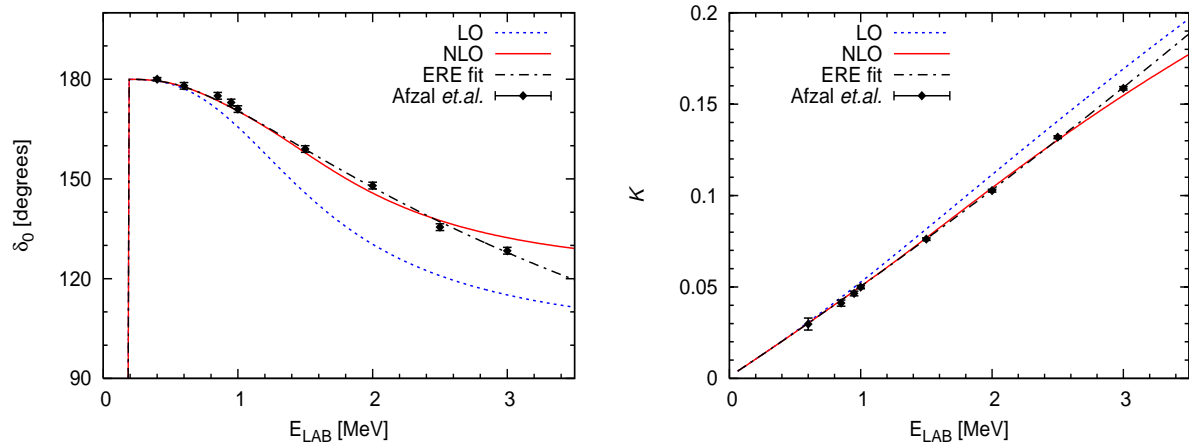


FIG. 1: Left panel: S -wave phase shift δ_0^c as a function of the laboratory energy E_{LAB} . The EFT results in LO and NLO are given by the (blue) dotted and (red) solid lines, respectively. Our ERE fit using Eq. (17) is given by the dash-dotted line and the empirical phase shifts [14] as (black) solid circles with error bars. Right panel: analogous results for the Landau-Smorodinsky K -function.

In LO, the two parameters a_0 and \tilde{r}_0 can be obtained from a fit to the resonance position and width. At NLO, scattering data are needed to determine $\tilde{\mathcal{P}}_0$.

Figure 1 shows the results of our fit to the available S -wave phase shifts below $E_{LAB} = 3$ MeV, including the resonance position and width. The latter control the steep rise of the phase shift at very low energies. In the region above the resonance, where scattering data are shown, the LO curve is a prediction, which is consistent with the first few points but then moves away from the data. The NLO curve has an extra parameter, which here was determined from a global χ^2 -fit to scattering data shown. As expected from a convergent expansion, the description of the low-energy data improves with increasing order. At about 3 MeV and above, higher-order contributions are expected to be significant, as suggested by the discussion on the relevant scales and manifest in the growing difference between the NLO curve and both LO curve and data points. Also shown are results from a fit using the conventional ERE formula, Eq. (17), in order to stress the differences between this and our EFT approach. The ERE formula includes some of the contributions of higher order in the EFT.

In Table I we give the values of ERE parameters that we extract from the fits in Fig. 1, and compare them with the values [13] obtained from effective range theory. At LO, a_0 and r_0 come out consistent with the values given in Ref. [13], r_0 in particular. The changes due to NLO corrections, however, worsen this initial LO agreement. The reason for this deviation is most likely due to the calculation of the width constraint in Ref. [13]. Its Eq. (4) reads

$$\frac{dh}{dk^2}(\eta_R) - \frac{1}{\mu\Gamma(E_R)} \frac{\pi}{e^{2\pi k_C/k_R} - 1} = \frac{1}{4k_C} (r_0 - \mathcal{P}_0 k_R^2), \quad (24)$$

where $h(\eta) \equiv \text{Re}[H(\eta)]$. Following this reference's procedure, we were able to reproduce the quoted value of the width (6.4 eV) only when $dh(\eta_R)/dk^2$ was approximated by $1/12k_C^2$ [see Eq. (15)]. This amounts to ignoring the electromagnetic piece of $\tilde{\mathcal{P}}_0$ in Eq. (23), which is inconsistent since the strong piece contributes at the same order. It explains why the value for r_0 in Ref. [13] agrees quite well with ours at LO but disagrees at NLO. With this larger

\tilde{r}_0 , one can also understand why Ref. [13] obtains a smaller a_0 (see the following discussion on the scaling of a_0). When we repeated Ref. [13]’s procedure including the width constraint consistently, we obtained essentially the same values as in our EFT fits. This updated ERE fit is also shown in Table I.

In agreement with our expectations, the effective range shows a natural size, $r_0 \sim 1/(180 \text{ MeV})$. The shape parameter also has a natural size $\mathcal{P}_0 \sim 1/(170 \text{ MeV})^3$ at NLO which is in agreement with our *a priori* estimate. The relative errors in a_0 and \tilde{r}_0 at LO are estimated to be of the order of the EFT parameter expansion, $M_{lo}/M_{hi} \sim 1/7 \approx 15\%$. At NLO, they are essentially given by the precision of the most recent measurement of the resonance width [18], which lies between 4–5%. The uncertainty in $\tilde{\mathcal{P}}_0$, given by the χ^2 -fit, is of the same order. Note that the small relative error in r_0 compared to the one in \tilde{r}_0 is due to the former being an order of magnitude larger than the latter, as we discuss below. The NLO errors found here are a factor of two smaller than the ones obtained by Ref. [13].

One should stress that the accurate value of the resonance width, $\Gamma_R = 5.57 \pm 0.25 \text{ eV}$, imposes tight constraints on our fits, through a_0 and r_0 . There is a significant improvement in our NLO fit and overall agreement with data, but the theoretical curve is not able to cross the error bands of all scattering points below 3 MeV, as reflected in a $\chi^2/\text{datum} \simeq 4$. In principle, a better agreement should be achieved by an N²LO calculation. However, that introduces an extra parameter that is mostly determined by the scattering data, and this agreement could mask any possible inconsistencies that the phase shifts might have with the resonance parameters. The high NLO χ^2/datum suggests that the resonance width and the S -wave scattering data set are not compatible with each other or, at least, one of them has overestimated precision. As a test we performed fits to scattering data without the input from the resonance width, within our NLO EFT and the conventional ERE framework. In both cases, description of S -wave phase shifts is much better but the resonance width is underpredicted, $\Gamma_R = 4.9 \pm 0.6 \text{ eV}$ with ERE and $\Gamma_R = 2.87 \pm 0.23 \text{ eV}$ with EFT. The ERE result is still consistent with the measured Γ_R thanks to its large error bar. In EFT, where lower-energy data have higher priority, the discrepancy is amplified. The problem is even more pronounced if the fit is performed using data up to 2.5 MeV instead of 3 MeV: the results $\Gamma_R = 4.2 \pm 0.6 \text{ eV}$ with ERE and $\Gamma_R = 2.93 \pm 0.34 \text{ eV}$ with EFT fall beyond the quoted experimental error bars. Oddly, this tendency continues as one lowers the upper limit in the fit. Reanalyses of the existing low-energy data or even new measurements seem necessary to resolve this discrepancy.

An astonishing feature of the $\alpha\alpha$ system is the very large magnitude of a_0 , even if compared to the large scattering length observed in the two-nucleon system. The latter is evidence of a fine-tuning in the QCD parameters, which gives rise to an anomalously low

	a_0 (10^3 fm)	r_0 (fm)	\mathcal{P}_0 (fm^3)
LO	−1.80	1.083	—
NLO	-1.92 ± 0.09	1.098 ± 0.005	-1.46 ± 0.08
ERE (our fit)	-1.92 ± 0.09	1.099 ± 0.005	-1.62 ± 0.08
ERE [13]	-1.65 ± 0.17	1.084 ± 0.011	-1.76 ± 0.22

TABLE I: ERE parameters extracted from EFT fits in the first two orders, compared with values from two ERE fits, our own and Ref. [13]’s.

momentum scale. (This fine-tuning can be seen as the proximity of the observed pion mass to the critical value ~ 200 MeV where the NN bound states have zero energy [27, 38] and the triton displays the Efimov effect [39].) Certainly this fine-tuning scale propagates to heavier systems. However, the enormous value of a_0 in the $\alpha\alpha$ system is suggestive of a more dramatic fine-tuning, with electromagnetic interactions playing a crucial role.

The parameters of the 0^+ resonance are indeed quite surprising. As we remarked, this resonance is associated with two poles of T_{CS} , the momenta of which are much smaller in magnitude than k_C . As a consequence, there is an exponential suppression of the width, which is evident in Eq. (23). Yet, the width is somewhat *large* given the position of the resonance. It is remarkable that in order to fit both the resonance position and width one needs $\tilde{r}_0 \simeq -0.13$ fm, nearly a factor 10 smaller in magnitude than the Coulomb contribution to the energy-dependent term, $-1/3k_C \simeq -1.2$ fm. That is, although both $r_0 \sim 1$ fm and $1/3k_C \sim 1$ fm as expected from dimensional analysis, they approximately cancel producing a balance that is about 10% of either. This balance would itself have natural size if the width were a factor of 10 smaller than measured, or else if k_R were 15% larger. Instead, the existing cancellation effectively leads to either $|\tilde{r}_0| \sim 1/\mu$ or $|\tilde{r}_0| \sim M_{lo}/M_{hi}^2$.

Since the position of the resonance determines to a first approximation $a_0\tilde{r}_0$, the seemingly accidental cancellation in \tilde{r}_0 translates into an exceptionally large a_0 , which is effectively $|a_0| \sim \mu/M_{lo}^2$ or $|a_0| \sim M_{hi}^2/M_{lo}^3$. The Coulomb-modified parameter $\Delta^{(R)}$ is thus suppressed by another power of M_{lo}/M_{hi} compared to the assumed scaling when Coulomb interactions are turned off.

The values of ERE parameters show that, as anticipated by the power counting we proposed, the strong-interaction effective-range term is comparable to both the scattering-length term and the electromagnetic H . A power counting based on the scalings appropriate for NN scattering would instead miss the resonance in LO unless one also counted $3k_C$ as M_{lo} , which is a numerical stretch. Even so, the width would be far off, since $1/3k_C \gg |\tilde{r}_0|$, and convergence questionable.

Although the results presented in this section were based on Eq. (19), and thus assumed the validity of the expansion (15), we have checked that no qualitative changes arise if one bases the EFT fits on Eq. (16) instead. In the latter case, one is simply retaining at each order some terms that truly belong to higher orders, at the cost of much less transparent analytical expressions.

V. CONCLUSION

In this paper, we have studied $\alpha\alpha$ interactions within the framework of halo/cluster EFT. From this perspective, the $\alpha\alpha$ system is most extraordinary.

EFT is model independent to the extent that includes all interactions allowed by known symmetries. It is equivalent in the $\alpha\alpha$ system to a truncation of the ERE. The halo EFT can be viewed as a formulation of the ERE that can be used for other systems made of shallow-bound alpha particles and, together with results from Refs. [5, 6, 7], also nucleons.

We have designed a power-counting scheme that seems realistic for the $\alpha\alpha$ system, but requires even more fine-tuning than the one in the NN system. It assumes that the parameter Δ in the EFT Lagrangian scales as M_{lo}^2/μ in the absence of the Coulomb interaction. Interesting in this scenario is the fact that at LO without Coulomb the ${}^8\text{Be}$ system would exhibit conformal invariance and ${}^{12}\text{C}$ would display an exact Efimov spectrum. These exact features are broken by the Coulomb interaction but some remnants of this behavior are

manifest in the experimental spectra, such as the shallowness of the 0^+ ^8Be resonance.

We have incorporated two new ideas in the halo/cluster EFT. The most effective way of implementing an EFT with resonances seems to be an expansion around the resonance pole, since it avoids the need for multiple kinematical fine-tunings and improves convergence. Our study was significantly simplified by treating the Coulomb function $H(\eta)$ in a power series expansion in k/k_C . This simplification may be very relevant when treating interactions with several alpha-particle clusters.

We made use of the precise measurements of the 0^+ resonance properties [18], together with the (rather old) existing S -wave scattering phase shifts [8] in order to produce LO and NLO fits that fix our ERE parameters. The result is in slight disagreement with Ref. [13], probably due to an approximation made in its calculation of the width. The uncertainties in our ERE parameters are smaller by a factor of two in comparison with this reference. A systematic improvement is seen in the theoretical phase shifts, and reasonably good overall description is obtained at NLO. Yet, the rather high χ^2 when the resonance width is fitted and the deterioration of the calculated width as one restricts the fit to lower-energy scattering data suggest that either the resonance width or the S -wave phase shifts have overestimated precision.

Despite the phenomenological success of the proposed power counting, the necessary cancellations between strong and Coulomb interactions, which seem accidental, are puzzling. In the absence of Coulomb interactions, the regulator-dependent part of the bare dimeron mass Δ is $\mathcal{O}(M_{hi}^2/\mu)$. As we can see from Eq. (12), the electromagnetic κ -dependent pieces do not change this expectation, since they are $\sim 2k_C\mu g^2/2\pi = \mathcal{O}(M_{hi}^2/\mu)$. Therefore, barring cancellations between the finite pieces of Δ and loops, we would expect the renormalized mass $\Delta^{(R)}$ to have the same size, which would set a scale for $|a_0|$ at $\mathcal{O}(1/M_{hi}) \sim 1/2k_C \simeq 2$ fm. Yet, the observed resonance energy (together with a natural-sized effective range \tilde{r}_0) tells us that $\Delta^{(R)} = \mathcal{O}(M_{lo}^2/\mu)$. A similar scaling for $\Delta^{(R)}$ emerges in $n\alpha$ scattering [5, 6], but here we need a further cancellation between the finite pieces in Δ and Coulomb loops. This brings $|a_0|$ up by two orders of magnitude, or more than two inverse powers of the expansion parameter $M_{lo}/M_{hi} \sim 1/7$, to $\mathcal{O}(M_{hi}/M_{lo}^2) \simeq 100$ fm.

Uncomfortable as this fine-tuning by a factor of nearly 100 in the energy-independent part of the amplitude T_{CS} might be, it is not the whole story. As we have shown, both the resonance width and the higher-energy phase shifts require a fine-tuning also in the energy dependence of the amplitude. This $\sim 90\%$ additional cancellation (together with the observed resonance energy) further enhances $|a_0|$ by another factor of 10, or about another inverse power of M_{lo}/M_{hi} , leading effectively to $\mathcal{O}(M_{hi}^2/M_{lo}^3) \simeq 700$ fm, which is indeed the order of magnitude we obtain in our fit. This fine-tuning of a factor of ~ 1000 in $\alpha\alpha$ completely overshadows the fine-tuning of ~ 10 —from m_π (or from the pion decay constant $f_\pi \simeq 92$ MeV) down to $1/|a_0| \simeq 8$ MeV—in the NN 1S_0 channel. It has important consequences: for example, if the strong-interaction effective range r_0 were just 15-20% larger it would make the ground state of ^8Be bound, presumably with far-reaching effects in nucleosynthesis.

This context frames a fascinating picture for the $\alpha\alpha$ system: a nearly conformally invariant system that is plagued by cancellations between strong and Coulomb interactions. Of course, fine-tuning has long been discussed in nuclear physics, but usually in connection to the position of the Hoyle state of ^{12}C (see, for example, Ref. [40]). An immediate question is to which extent the latter arises from the fine-tunings we discussed here.

Together with previous and ongoing work on the $n\alpha$ [5, 6] and $p\alpha$ systems [7], our results

provide a framework for the description of cluster states in nuclei using EFT, which can be seen as a generalization of the ERE to systems that involve more than two bodies. An important extension of this work is to systems of more than two alpha particles. The strong $\alpha\alpha$ interaction obtained here, together with an exact treatment of the Coulomb interaction, should provide the necessary ingredients. Since $k_C/k_R \sim 3$ as discussed above, one might be able to simplify the calculation of Coulomb effects by developing a perturbation scheme in powers of k_R/k_C from the start. Moreover, we conjecture that the ^{12}C Hoyle state is a remnant of an Efimov state that appears in the unitary limit. More complex α -cluster systems could also be studied with the EFT presented here.

Acknowledgments

We would like to thank Carlos Bertulani for useful discussions and encouragement. RH has also benefited from discussions with Andreas Nogga, and UvK with Brett Carlson, Tobias Frederico, Boris Gelman, and Manuel Malheiro. This research was supported in part by the Bundesministerium für Bildung und Forschung under contract number 06BN411 (RH, HWH), by the U.S. Department of Energy (UvK), by the Nederlandse Organisatie voor Wetenschappelijk Onderzoek (UvK), and by Brazil's FAPESP under a Visiting Professor grant (UvK). UvK would like to thank the hospitality of the Kernfysisch Versneller Instituut at Rijksuniversiteit Groningen, the Instituto de Física Teórica of the Universidade Estadual Paulista, and the Instituto de Física of the Universidade de São Paulo, where part of this work was carried out.

APPENDIX A: COULOMB GREEN'S FUNCTION AND EFT

The scattering amplitude for two particles in their center-of-mass (CM) system interacting via Coulomb and a short-range interaction is given by [35]

$$T = T_C + T_{CS} = \langle \chi_{k'}^{(-)} | V_C | \mathbf{k} \rangle + \langle \chi_{k'}^{(-)} | V_S | \Psi_k^{(+)} \rangle, \quad (\text{A1})$$

where $|\mathbf{k}\rangle$, $|\chi_k^{(+/-)}\rangle$, and $|\Psi_k^{(+/-)}\rangle$ represent free and (incoming/outgoing) states of momentum \mathbf{k} for pure-Coulomb and Coulomb-distorted short-range interactions, respectively, while V_C (V_S) is the Coulomb (short-range) interaction operator. In coordinate space, the Coulomb wave functions can be written as [23]

$$\langle \mathbf{r} | \chi_k^{(\pm)} \rangle \equiv \chi_k^{(\pm)}(\mathbf{r}) = e^{-\frac{\eta\pi}{2}} \Gamma(1 \pm i\eta) M(\mp i\eta, 1; \pm ikr - i\mathbf{k} \cdot \mathbf{r}) e^{i\mathbf{k} \cdot \mathbf{r}}, \quad (\text{A2})$$

where $M(a, b; z)$ is the Kummer function. From $M(a, b; 0) = 1$ [36], one obtains the important properties

$$\chi_{k'}^{(\pm)*}(0) \chi_k^{(\pm)}(0) = e^{-\pi\eta} \Gamma(1 \mp i\eta) \Gamma(1 \pm i\eta) = \frac{2\pi\eta}{e^{2\pi\eta} - 1} \equiv C_\eta^2, \quad (\text{A3})$$

$$\chi_{k'}^{(\mp)*}(0) \chi_k^{(\pm)}(0) = e^{-\pi\eta} \Gamma(1 \pm i\eta)^2 = C_\eta^2 e^{\pm 2i\sigma_0}, \quad (\text{A4})$$

where σ_0 is the Coulomb phase shift for the partial wave $l = 0$. The general expression for the Coulomb phase shift,

$$\sigma_l = \arg \Gamma(l + 1 + i\eta) = \frac{1}{2i} \ln \left[\frac{\Gamma(l + 1 + i\eta)}{\Gamma(l + 1 - i\eta)} \right], \quad (\text{A5})$$

is defined from the partial-wave expansion of the pure-Coulomb amplitude

$$T_C = -\frac{2\pi}{\mu} \sum_{l=0}^{\infty} (2l+1) \frac{(e^{2i\sigma_l} - 1)}{2ik} P_l(\cos \theta) = -\frac{2\pi}{\mu} f_C(\theta). \quad (\text{A6})$$

The explicit solution

$$f_C(\theta) = -\frac{\eta^2}{2k_C} \csc^2 \theta/2 \exp \left[i\eta \ln(\csc^2 \theta/2) + 2i\sigma_0 \right] \quad (\text{A7})$$

leads to the well-known Mott scattering cross section, $\sigma_M = |f_C(\theta) + f_C(\pi - \theta)|^2$, which holds at very low energies.

The main ingredient in the calculation of the Coulomb-distorted short-range amplitude is the Coulomb Green's function at energy E ,

$$G_C^{(\pm)}(E) = \frac{1}{E - H_C \pm i\epsilon} = 2\mu \int \frac{d^3q}{(2\pi)^3} \frac{|\chi_q^{(\pm)}\rangle \langle \chi_q^{(\pm)}|}{2\mu E - \mathbf{q}^2 \pm i\epsilon}. \quad (\text{A8})$$

Using the Lippmann-Schwinger equation, one is able to express $|\Psi_k^{(\pm)}\rangle$ in terms of multiple insertions of the operator $G_C^{(\pm)}V_S$ acting on the Coulomb states $|\chi_k^{(\pm)}\rangle$ [23], allowing the amplitude to be written as the sum

$$T_{CS} = \sum_{n=0}^{\infty} \langle \chi_{k'}^{(-)} | V_S (G_C^{(\pm)} V_S)^n | \chi_k^{(+)} \rangle. \quad (\text{A9})$$

This amplitude can be decomposed into partial waves,

$$T_{CS} = \sum_{l=0}^{\infty} T_l P_l(\cos \theta), \quad T_l = -\frac{2\pi}{\mu} (2l+1) \frac{e^{2i\sigma_l}}{k(\cot \delta_l^c - i)}, \quad (\text{A10})$$

in terms of the ‘‘Coulomb-corrected’’ phase shifts δ_l^c .

If the deviation from the Mott cross section is mostly S wave, then the calculation of T_{CS} proceeds from the Lagrangian (1) similarly to Ref. [23]. The purely strong matrix element $\langle \mathbf{p}' | V_S | \mathbf{p} \rangle$ is defined as the amplitude $t_d = g^2 D_d(E; \mathbf{0})$ for $\alpha\alpha$ scattering via a bare dimeron two-point function, with the external legs amputated, evaluated in the CM:

$$\langle \mathbf{p}' | V_S | \mathbf{p} \rangle = g^2 D_d(E; \mathbf{0}) = \frac{\sigma g^2}{E - \Delta + i\epsilon}. \quad (\text{A11})$$

Explicit evaluation of Eq. (A9) using Eqs. (A3), (A4), and (A11) then gives

$$T_{CS} = \frac{\sigma g^2}{E - \Delta + i\epsilon} C_\eta^2 e^{2i\sigma_0} \left[1 + \frac{\sigma g^2}{E - \Delta + i\epsilon} J_0(E) + \left(\frac{\sigma g^2}{E - \Delta + i\epsilon} J_0(E) \right)^2 + \dots \right]. \quad (\text{A12})$$

This resummation of the Coulomb exchanges is illustrated in Fig. 2. It leads to

$$T_{CS} = -\frac{2\pi}{\mu} C_\eta^2 e^{2i\sigma_0} \left[\sigma \frac{2\pi\Delta}{\mu g^2} - \sigma \frac{2\pi E}{\mu g^2} - i\epsilon + \frac{2\pi}{\mu} J_0(E) \right]^{-1}, \quad (\text{A13})$$

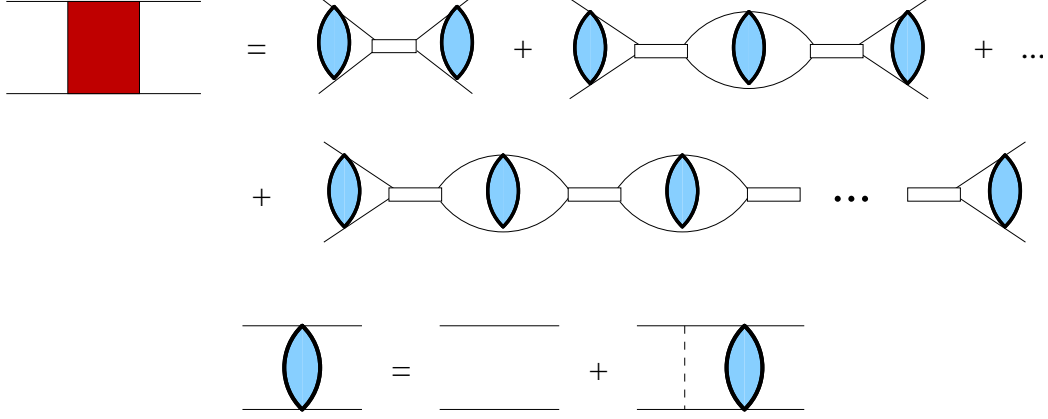


FIG. 2: Resummation for the LO expression of T_{CS} , represented by the (red) shaded rectangle. The double line stands for the dimeron propagator. The (blue) shaded ellipse represents the propagation in the presence of Coulomb photons (dashed line) but absence of a dimeron.

where J_0 is given by

$$J_0(E) = -\frac{\mu}{2\pi} \left\{ \frac{\kappa}{D-3} + 2k_C \left[H(\eta) + \frac{1}{D-4} - \ln \left(\frac{\kappa\sqrt{\pi}}{2k_C} \right) - 1 + \frac{3}{2} C_E \right] \right\}, \quad (\text{A14})$$

with D the dimensionality of spacetime, κ the renormalization scale, $k_C = Z_\alpha^2 \alpha_{em} \mu = k\eta$, $C_E = 0.577\dots$ the Euler-Mascheroni constant, and

$$H(\eta) = \psi(i\eta) + \frac{1}{2i\eta} - \ln(i\eta) \quad (\text{A15})$$

in terms of the digamma function ψ , which obeys [36]

$$\text{Re}[\psi(i\eta)] = \text{Re}[\psi(1+i\eta)], \quad \text{Im}[\psi(i\eta)] = \frac{1}{2\eta} + \frac{\pi}{2} \coth \pi\eta. \quad (\text{A16})$$

The dimeron mass gets renormalized by the non-perturbative free-particle and Coulomb loops,

$$\sigma \frac{2\pi\Delta^{(R)}}{\mu g^2} = \sigma \frac{2\pi\Delta(\kappa)}{\mu g^2} - \frac{\kappa}{D-3} - 2k_C \left[\frac{1}{D-4} - \ln \left(\frac{\kappa\sqrt{\pi}}{2k_C} \right) - 1 + \frac{3}{2} C_E \right], \quad (\text{A17})$$

and T_{CS} finally becomes

$$T_{CS} = -\frac{2\pi}{\mu} C_\eta^2 e^{2i\sigma_0} \left[\sigma \frac{2\pi\Delta^{(R)}}{\mu g^2} - \sigma \frac{\pi}{\mu^2 g^2} k^2 - 2k_C H(\eta) \right]^{-1}. \quad (\text{A18})$$

[1] P.F. Bedaque and U. van Kolck, Ann. Rev. Nucl. Part. Sci. **52**, 339 (2002); E. Epelbaum, Prog. Nucl. Part. Phys. **57**, 654 (2006).

- [2] E. Braaten and H.-W. Hammer, Phys. Rept. **428**, 259 (2006).
- [3] I. Stetcu, B.R. Barrett, and U. van Kolck, Phys. Lett. **B653**, 358 (2007); I. Stetcu, B.R. Barrett, U. van Kolck, and J. Vary, Phys. Rev. A **76**, 063613 (2007).
- [4] B. Borasoy, E. Epelbaum, H. Krebs, D. Lee, and U.-G. Meißner, Eur. Phys. J. A **31**, 105 (2007).
- [5] C.A. Bertulani, H.-W. Hammer, and U. van Kolck, Nucl. Phys. **A712**, 37 (2002).
- [6] P.F. Bedaque, H.-W. Hammer, and U. van Kolck, Phys. Lett. **B569**, 159 (2003).
- [7] C.A. Bertulani, R. Higa, and U. van Kolck, in progress.
- [8] N.P. Heydenburg and G.M. Temmer, Phys. Rev. **104**, 123 (1956).
- [9] J.L. Russell, Jr., G.C. Phillips, and C.W. Reich, Phys. Rev. **104**, 135 (1956).
- [10] T.A. Tombrello and L.S. Senhouse, Phys. Rev. **129**, 2252 (1963).
- [11] C.M. Jones, G.C. Phillips, and P.D. Miller, Phys. Rev. **117**, 525 (1960).
- [12] T.A. Tombrello, Phys. Lett. **23**, 106 (1966).
- [13] G. Rasche, Nucl. Phys. **A94**, 301 (1967).
- [14] S.A. Afzal, A.A.Z. Ahmad, and S. Ali, Rev. Mod. Phys. **41**, 247 (1969).
- [15] D.R. Tilley, J.H. Kelley, J.L. Godwin, D.J. Millener, J.E. Purcell, C.G. Sheu, and H.R. Weller, Nucl. Phys. **A745**, 155 (2004).
- [16] K.W. Jones, D.J. Donahue, M.T. McEllistrem, R.A. Douglas, and H.T. Richards, Phys. Rev. **91**, 879 (1953).
- [17] J. Benn, E.B. Dally, H.H. Müller, R.E. Pixley, H.H. Staub, and H. Winkler, Nucl. Phys. **A106**, 296 (1967).
- [18] S. Wüstenbecker, H.W. Becker, H. Ebbing, W.H. Schulte, M. Berheide, M. Buschmann, C. Rolfs, G.E. Mitchell, and J.S. Schweitzer, Z. Phys. A **344**, 205 (1992).
- [19] D.B. Kaplan, Nucl. Phys. **B494**, 471 (1997).
- [20] U. van Kolck, arXiv:hep-ph/9711222, in *Proceedings of the Workshop on Chiral Dynamics 1997, Theory and Experiment*, ed. A. Bernstein, D. Drechsel, and T. Walcher (Springer-Verlag, Berlin, 1998); Nucl. Phys. **A645**, 273 (1999); D.B. Kaplan, M.J. Savage, and M.B. Wise, Phys. Lett. **B424**, 390 (1998); Nucl. Phys. **B534**, 329 (1998); J. Gegelia, Phys. Lett. **B429**, 227 (1998).
- [21] J.-W. Chen, G. Rupak, and M.J. Savage, Nucl. Phys. **A653**, 386 (1999).
- [22] D.R. Phillips, G. Rupak, and M.J. Savage, Phys. Lett. **B473**, 209 (2000).
- [23] X. Kong and F. Ravndal, Phys. Lett. **B450**, 320 (1999); Nucl. Phys. **A665**, 137 (2000); B.R. Holstein, Phys. Rev. D **60**, 114030 (1999); S. Ando, J.W. Shin, C.H. Hyun, and S.W. Hong, Phys. Rev. C **76**, 064001 (2007).
- [24] T. Mehen, I.W. Stewart, and M.B. Wise, Phys. Lett. **B474**, 145 (2000).
- [25] P.F. Bedaque, H.-W. Hammer, and U. van Kolck, Phys. Rev. Lett. **82**, 463 (1999); Nucl. Phys. **A646**, 444 (1999).
- [26] V. Efimov, Sov. J. Nucl. Phys. **12**, 589 (1971) [Yad. Fiz. **12**, 1080 (1970)]; Sov. J. Nucl. Phys. **29**, 546 (1979) [Yad. Fiz. **29**, 1058 (1979)].
- [27] S.R. Beane, P.F. Bedaque, K. Orginos, and M.J. Savage, Phys. Rev. Lett. **97**, 012001 (2006).
- [28] A.S. Jensen, K. Riisager, D.V. Fedorov, and E. Garrido, Rev. Mod. Phys. **76**, 215 (2004).
- [29] T. Frederico, M.T. Yamashita, and L. Tomio, Few-Body Syst. **38**, 57 (2006).
- [30] R. Álvarez-Rodríguez, A.S. Jensen, D.V. Fedorov, H.O.U. Fynbo, and E. Garrido, Phys. Rev. Lett. **99**, 072503 (2007); J. Phys. G **35**, 014010 (2008).
- [31] E. Ruiz Arriola, arXiv:0709.4134.
- [32] L.A. Barreiro, R. Higa, C.L. Lima, and M.R. Robilotta, Phys. Rev. C **57**, 2142 (1998).

- [33] S. Ando, Eur. Phys. J. **A33**, 185 (2007); S. Ando, J.W. Shin, C.H. Hyun, S.W. Hong, and K. Kubodera, arXiv:0801.4330.
- [34] J. Gasser, V.E. Lyubovitskij, and A. Rusetsky, Phys. Rept. **456**, 167 (2008).
- [35] M.L. Goldberger and K.M. Watson, *Collision Theory* (John Wiley and Sons, Inc., New York, 1967).
- [36] M. Abramowitz and I.A. Stegun (eds.), *Handbook of Mathematical Functions* (Dover Publications, Inc., New York, 1972).
- [37] L. Landau and Ya. Smorodinsky, J. Phys. Acad. Sci. U.S.S.R. **8**, 154 (1944).
- [38] S.R. Beane, P.F. Bedaque, M.J. Savage, and U. van Kolck, Nucl. Phys. **A700**, 377 (2002); S.R. Beane and M.J. Savage, Nucl. Phys. **A713**, 148 (2003); Nucl. Phys. **A717**, 91 (2003); E. Epelbaum, U.-G. Meißner, and W. Glöckle, Nucl. Phys. **A714**, 535 (2003); arXiv:nucl-th/0208040.
- [39] E. Braaten and H.-W. Hammer, Phys. Rev. Lett. **91**, 102002 (2003); E. Epelbaum, H.-W. Hammer, U.-G. Meißner, and A. Nogga, Eur. Phys. J. C **48**, 169 (2006); H.-W. Hammer, D.R. Phillips, and L. Platter, Eur. Phys. J. A **32**, 335 (2007).
- [40] H. Oberhummer, H. Krauss, K. Grün, T. Rauscher, H. Abele, P. Mohr, and G. Staudt, arXiv:nucl-th/9310016v1; H. Oberhummer, A. Csótó, and H. Schlattl, Science **289**, 88 (2000).